Nanoparticle modified monolithic materials

Mgr. Jana Krenkova, Ph.D.

Brno, 23. 11. 2017

Control of surface chemistry

- Preparation from functional monomers
  - polymerization
  - grafting

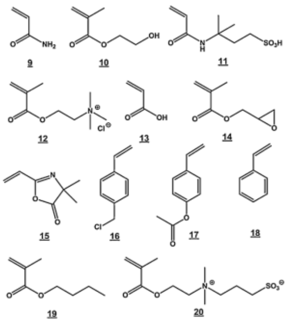

F. Svec, *J. Chromatogr. A* 2010, 1217, 902–924

Control of surface chemistry

- Modification of reactive monoliths

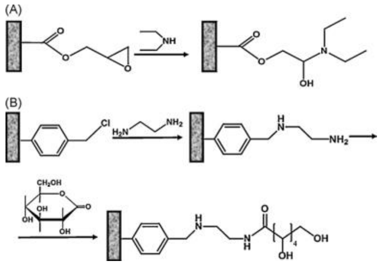

F. Svec, *J. Chromatogr. A* 2010, 1217, 902–924

Control of surface chemistry

- Attachment of nanomaterials

Nanomaterials
materials of which a single unit is sized (in at least one dimension) between 1 and 100 nanometers

Why nanomaterials?
selectivity – chromatography, sample preparation
surface area
ligands for immobilization of bioactive molecules

Modification of monoliths with nanoparticles

- embedding (encapsulation) of NPs in the monolithic matrix
  - simple and straightforward approach
  - distribution of NPs throughout the monolithic matrix
    limited accessibility of NPs for desired interactions
- attachment of nanoparticles to the surface of preformed monoliths
  - multistep approach
  - independent optimization of individual steps
    improved accessibility of NPs for desired interactions

Latex nanoparticles

Ion exchange chromatography - carbohydrates

monolith:
poly(BMA-co-EDMA-co-AMPS)

latex particles (60 nm diameter) with tertiary amine functionality

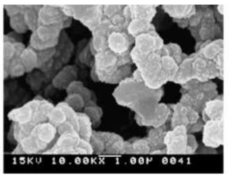

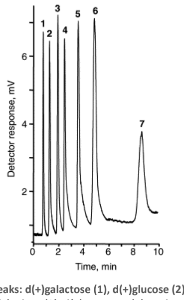

Peaks: d(+)galactose (1), d(+)glucose (2), d(+)xylose (3), d(+)mannose (4), maltose (5), d(−)fructose (6), sucrose (7).

BMA – butyl methacrylate, EDMA – ethylene dimethacrylate, AMPS - 2-acrylamido-2-methyl-1-propanesulfonic acid

Hilder et al. *J. Chrom. A* 2004 1053, 101

Gold nanoparticles

Citation synthesis

$HAuCl_4$ + trisodium citrate dihydrate

Au+3 ions are reduced to neutral gold atoms, where citrate ions act as both a reducing agent and a capping agent.

Colors of various sized monodispersed gold nanoparticles

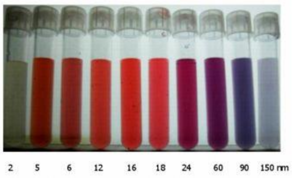

Gold nanoparticles

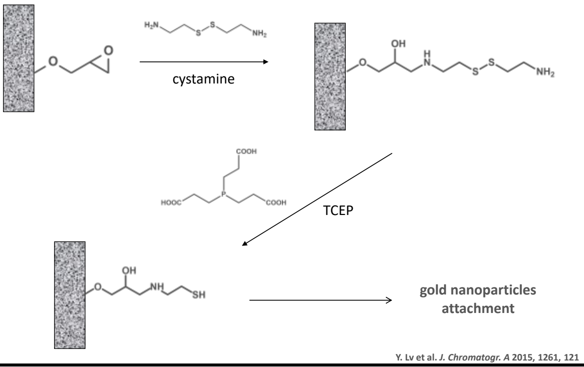

Y. Lv et al. *J. Chromatogr. A* 2015, 1261, 121

Gold nanoparticles

Cys-GMA monolith functionalized with 15 nm gold nanoparticles

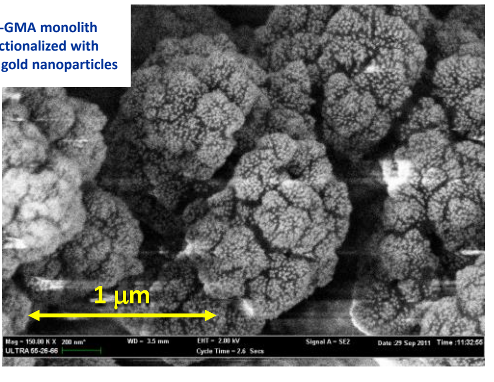

Gold nanoparticles

Thiol-containing peptide enrichment
Ligand exchange - various chromatographic modes

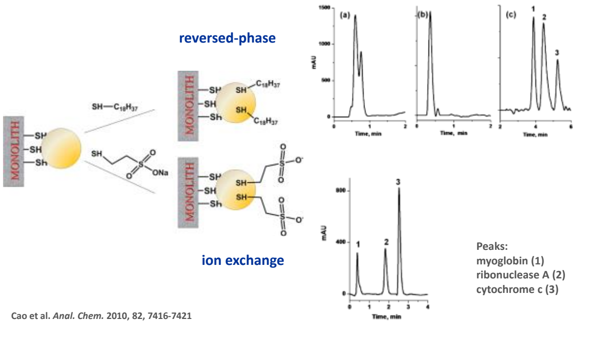

Peaks:
myoglobin (1)
ribonuclease A (2)
cytochrome c (3)

Cao et al. *Anal. Chem.* 2010, 82, 7416-7421

Gold nanoparticles

Lectin immobilization

Erythrina cristagalli lectin - galactose-selective lectin (ECL)

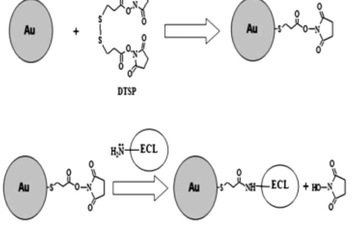

H. Alwael et al. *Analyst* 2011, 136, 2619

Gold nanoparticles

Lectin immobilization

Erythrina cristagalli lectin - galactose-selective lectin (ECL)

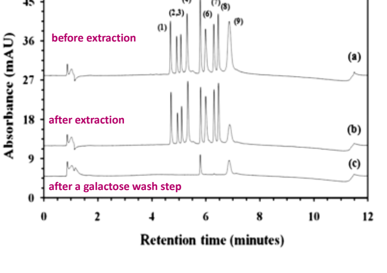

RP-LC/UV separation of protein mixture

Peaks:
(1) ribonuclease B
(2) insulin chain B
(3) insulin
(4) cytochrome C
(5) desialylated transferrin
(6) BSA
(7) carbonic anhydrase
(8) enolase
(9) desialylated thyroglobulin

H. Alwael et al. *Analyst* 2011, 136, 2619

Fullerenes

molecule of carbon in the form of a hollow sphere, ellipsoid, tube, and many other shapes

spherical fullerenes - buckyballs

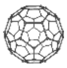

cylindrical fullerenes - carbon nanotubes or buckytubes

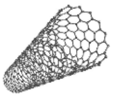

C_{60} in solution

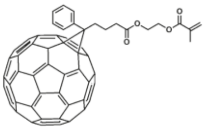

[6,6]-phenyl-C61-butyric acid 2-hydroxyethylmethacrylate ester

Fullerenes

Reversed-phase chromatography

Separation of alkylbenzenes

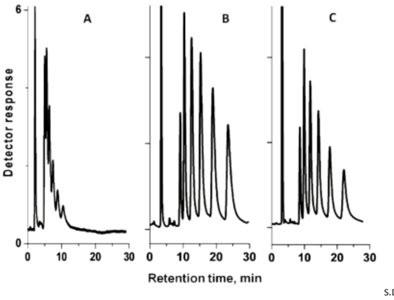

110 000 plates/m for the retained benzene

Conditions: column 53 mm x 100 µm i.d., flow rate 0.15 µL/min, UV detection at 254 nm; (A) mobile phase 50:50 vol % acetonitrile-water; (B) mobile phase 50:50 vol % acetonitrile-water; (C) mobile phase 47.5:2.5:50 vol % acetonitrile-tetrahydrofuran-water; peaks in order of elution: uracil, benzene, toluene, ethylbenzene, propylbenzene, butylbenzene, and amylbenzene

S.D. Chambers et al. *Anal. Chem.* 2011, 83, 9478

Carbon nanotubes

Reversed-phase chromatography

Multi-wall nanotubes

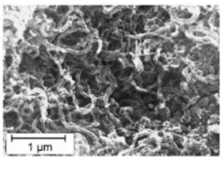

Separation of alkylbenzenes

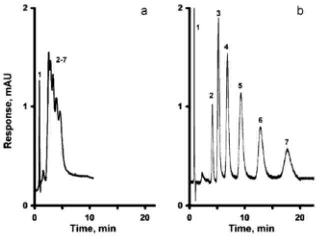

Conditions: column, 180mm × 100 µm ID, mobile phase 45% acetonitrile–5% THF–50% water, flow rate 1µL/min, UV detection at 254 nm; peaks: uracil (1), benzene (2), toluene (3), ethylbenzene (4), propylbenzene (5), butylbenzene (6), and amylbenzene (7).

S.D. Chambers et al. *J. Chromatogr. A* 2011, 1218, 2546

Metal-organic frameworks (MOF)

compounds consisting of metal ions or clusters coordinated to organic molecules to form one-, two-, or three-dimensional structures

properties
- superlative porosity
- wide chemical tunability
- high stability

applications
- gas storage
- gas separation
- catalysis

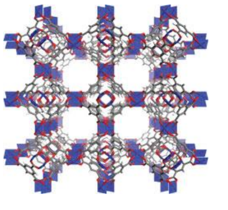

MOFs in monolithic materials
- preparation in situ
- admixing preformed MOFs

Metal-organic frameworks (MOF)

Preparation *in situ*

monolith containing carboxylic acid functionalities

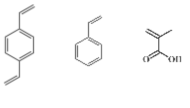

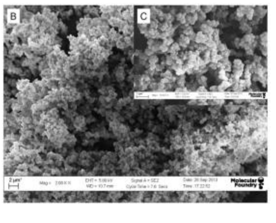

synthesis of MIL-100

inorganic metal ions - $FeCl_3$

organic ligand - 1,3,5-benzenetricarboxylic acid (BTC)

A. Saeed et al. *Adv. Funct. Mater.* 2014, 24, 5790

Metal-organic frameworks (MOF)

layer-by-layer growth (30 cycles)

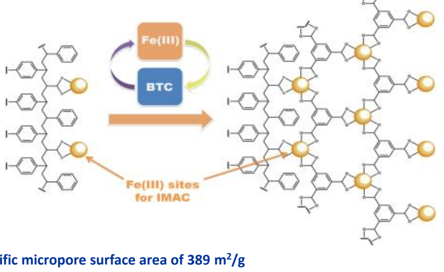

high specific micropore surface area of 389 m^2/g

(original polymer monolith – surface area of 106 m^2/g)

A. Saeed et al. *Adv. Funct. Mater.* 2014, 24, 5790

Metal-organic frameworks (MOF)

Phosphopeptide enrichment (IMAC) - MALDI/MS

analysis of nonfat milk

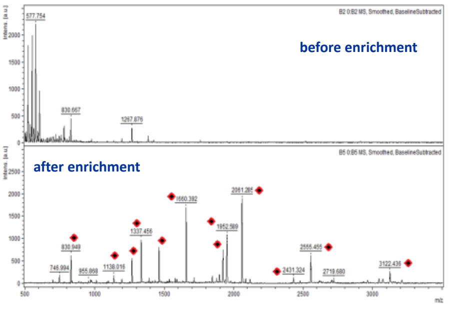

A. Saeed et al. *Adv. Funct. Mater.* 2014, 24, 5790

Titanium and zirconium oxide nanoparticles

Metal oxide affinity chromatography (MOAC)

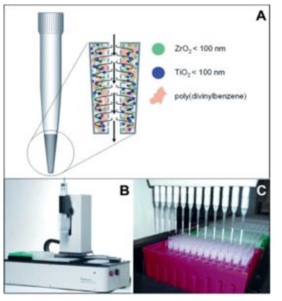

MALDI mass spectrum obtained from *in vitro* phosphorylated ERK1 digest before (A) and after enrichment with poly(DVB)-TiO2/ZrO2 microcolumns (B)

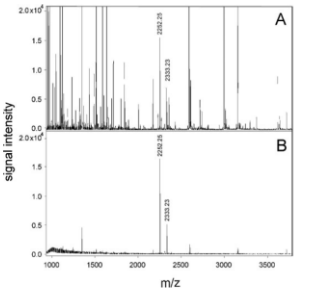

M. Rainer et al. *Proteomics* 2008, *8*, 4593

Iron oxide nanoparticles

- 200 µL polypropylene pipette tips
- modification of the inner wall by **methyl methacrylate/ethylene dimethacrylate**
- **poly(2-hydroxyethyl methacrylate-co-ethylene dimethacrylate)**
  5 µL monolithic bed prepared by UV-initiated polymerization
- UV-photografting of **[3-(methacroylamino)propyl]trimethyl-ammonium chloride** on the pore surface of the monolith
- attachment of **20 nm citrate stabilized iron oxide NPs** on the quaternary amine functionalized monolith

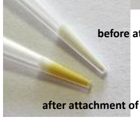

$Fe^{3+} + Fe^{2+} + OH^- \rightarrow Fe_3O_4 + H_2O$ $\xrightarrow{\text{oxidation}}$ $\gamma\text{–}Fe_2O_3$

$n(Fe^{2+})/n(Fe^{3+})=1/2$
pH>10

Krenkova J., Foret F. *Anal. Bioanal. Chem.* 2013, *405*, 2175

Hydroxyapatite nanoparticles

- 200 µL polypropylene pipette tips
- modification of the inner wall by **methyl methacrylate/ethylene dimethacrylate**
- **poly(2-hydroxyethyl methacrylate-co-ethylene dimethacrylate)** with embedded **hydroxyapatite NPs** (nanorods – 50 x 150 nm)
  5 µL monolithic bed prepared by UV-initiated polymerization

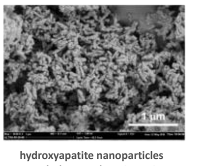

hydroxyapatite nanoparticles
morphology: rods - 50 x 150 nm
surface area: 115 m2/g

Krenkova J., Foret F. *Anal. Bioanal. Chem.* 2013, *405*, 2175

Phosphopeptide enrichment – MALDI/MS analysis

β-casein: 224 amino acid residues
5 phosphorylation sites

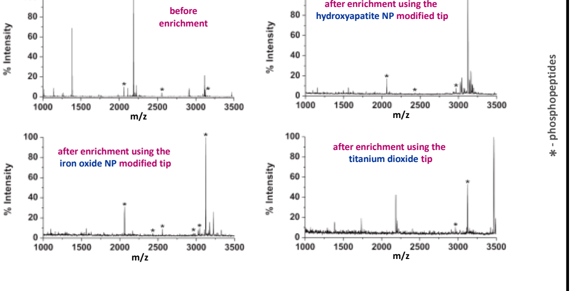

Krenkova J., Foret F. *Anal. Bioanal. Chem.* 2013, *405*, 2175

Institute of Analytical Chemistry of the CAS

Veveří 967/97
602 00 Brno

www.iach.cz

Dana Moravcova – moravcova@iach.cz

Jana Krenkova – krenkova@iach.cz